Beta-caryophyllene is a dietary cannabinoid

Jürg Gertsch*†, Marco Leonti‡§, Stefan Raduner*§, Ildiko Racz¶, Jian-Zhong Chen‖, Xiang-Qun Xie‖, Karl-Heinz Altmann*, Meliha Karsak¶, and Andreas Zimmer¶

*Institute of Pharmaceutical Sciences, Department of Chemistry and Applied Biosciences, Eidgenössische Technische Hochschule (ETH) Zurich, 8092 Zürich, Switzerland; ‡Dipartimento Farmaco Chimico Tecnologico, University of Cagliari, 01924 Cagliari, Italy; ¶Department of Molecular Psychiatry, University of Bonn, 53115 Bonn Germany; and ‖Department of Pharmaceutical Sciences, University of Pittsburgh, Pittsburgh, PA 15260

Edited by L. L. Iversen, University of Oxford, Oxford, United Kingdom, and approved May 6, 2008 (received for review April 14, 2008)

The psychoactive cannabinoids from *Cannabis sativa* L. and the arachidonic acid-derived endocannabinoids are nonselective natural ligands for cannabinoid receptor type 1 (CB_1) and CB_2 receptors. Although the CB_1 receptor is responsible for the psychomodulatory effects, activation of the CB_2 receptor is a potential therapeutic strategy for the treatment of inflammation, pain, atherosclerosis, and osteoporosis. Here, we report that the widespread plant volatile (*E*)-β-caryophyllene [(*E*)-BCP] selectively binds to the CB_2 receptor ($K_i = 155 \pm 4$ nM) and that it is a functional CB_2 agonist. Intriguingly, (*E*)-BCP is a common constituent of the essential oils of numerous spice and food plants and a major component in *Cannabis*. Molecular docking simulations have identified a putative binding site of (*E*)-BCP in the CB_2 receptor, showing ligand π–π stacking interactions with residues F117 and W258. Upon binding to the CB_2 receptor, (*E*)-BCP inhibits adenylate cylcase, leads to intracellular calcium transients and weakly activates the mitogen-activated kinases Erk1/2 and p38 in primary human monocytes. (*E*)-BCP (500 nM) inhibits lipopolysaccharide (LPS)-induced proinflammatory cytokine expression in peripheral blood and attenuates LPS-stimulated Erk1/2 and JNK1/2 phosphorylation in monocytes. Furthermore, peroral (*E*)-BCP at 5 mg/kg strongly reduces the carrageenan-induced inflammatory response in wild-type mice but not in mice lacking CB_2 receptors, providing evidence that this natural product exerts cannabimimetic effects *in vivo*. These results identify (*E*)-BCP as a functional nonpsychoactive CB_2 receptor ligand in foodstuff and as a macrocyclic antiinflammatory cannabinoid in *Cannabis*.

Cannabis | CB2 cannabinoid receptor | foodstuff | inflammation | natural product

Plant essential oils are typically composed of volatile aromatic terpenes and phenylpropanoids. These lipophilic volatiles freely cross cellular membranes and serve various ecological roles, like plant-insect interactions (1, 2). The sesquiterpene (*E*)-β-caryophyllene [(*E*)-BCP] (Fig. 1) is a major plant volatile found in large amounts in the essential oils of many different spice and food plants, such as oregano (*Origanum vulgare* L.), cinnamon (*Cinnamomum* spp.) and black pepper (*Piper nigrum* L.) (3–5). In nature, (*E*)-BCP is usually found together with small quantities of its isomers (*Z*)-β-caryophyllene [(*Z*)-BCP or isocaryophyllene] and α-humulene (formerly α-caryophyllene) or in a mixture with its oxidation product, BCP oxide (Fig. 1). Because of its weak aromatic taste, (*E*)-BCP is commercially used as a food additive and in cosmetics (6). (*E*)-BCP is also a major component (up to 35%) in the essential oil of *Cannabis sativa* L (7). Although *Cannabis* contains >400 different secondary metabolites, including >65 cannabinoid-like natural products, only Δ^9-tetrahydrocannabinol (THC), Δ^8-tetrahydrocannabinol, and cannabinol have been reported to activate cannabinoid receptor types 1 (CB_1) and 2 (CB_2) (8). Here, we show that the essential oil component (*E*)-BCP selectively binds to the CP55,940 binding site (i.e., THC binding site) in the CB_2 receptor, leading to cellular activation and antiinflammatory effects.

CB_1 and CB_2 cannabinoid receptors are GTP-binding protein (G protein) coupled receptors that were first cloned in the early 1990s (9, 10). Although the CB_1 receptor is expressed in the central nervous system and in the periphery, the CB_2 receptor is primarily found in peripheral tissues (11). *In vivo*, CB receptors are activated by arachidonic acid-derived endocannabinoids, such as 2-arachidonoyl ethanolamine (anandamide or AEA) and 2-arachidonoylglycerol (2-AG) (12, 13). In addition to a wide range of primarily CB_1 receptor-mediated physiological effects on the central nervous system, different cannabinoid ligands have been reported to modulate immune responses (14). In particular, CB_2 receptor ligands have been shown to inhibit inflammation and edema formation (15), exhibit analgesic effects (16), and play a protective role in hepatic ischemia-reperfusion injury (17). In the gastrointestinal tract, CB_2 receptor agonists have been shown to prevent experimental colitis by reducing inflammation (18). Moreover, the CB_2 receptor has been described as a potential target for the treatment of atherosclerosis (19) and osteoporosis (20). Consequently, CB_2 receptor-selective agonists that are devoid of the psychoactive side effects typically associated with CB_1 receptor activation are potential drug candidates for the treatment of a range of different diseases.

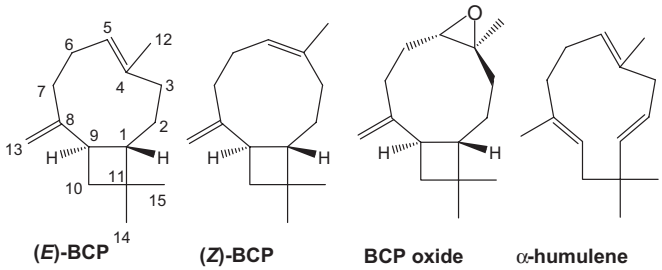

Fig. 1. Caryophyllane- and humulane-type sesquiterpenes found in *C. sativa* and numerous other plants. Shown are the chemical structures of the bicyclic sesquiterpenes (*E*)-β-caryophyllene, (*Z*)-β-caryophyllene, caryophyllene oxide, and the ring-opened isomer α-humulene (α-caryophyllene).

Results

Identification of CB_2 Receptor-Selective Ligands in *Cannabis* Essential Oil. In our ongoing search for new CB_2 cannabinoid receptor-selective ligands from natural sources, we observed that *C. sativa* essential oil (5 μg/ml) devoid of the classical cannabinoids strongly displaced the high-affinity radioligand [^{3}H]CP55,940 (21) from hCB_2 but not hCB_1 receptors [supporting information (SI) Fig. S1]. The same observation was made for a number of other essential oils, thus suggesting that *Cannabis* essential oil may contain CB_2

Author contributions: J.G. and M.K. designed research; J.G., M.L., S.R., I.R., and J.-Z.C. performed research; A.Z. contributed new reagents/analytic tools; J.G., X.-Q.X., K.-H.A., M.K., and A.Z. analyzed data; and J.G. wrote the paper.

The authors declare no conflict of interest.

This article is a PNAS Direct Submission.

†To whom correspondence should be addressed. E-mail: juerg.gertsch@pharma.ethz.ch.

§M.L. and S.R. contributed equally to this work.

This article contains supporting information online at www.pnas.org/cgi/content/full/0803601105/DCSupplemental.

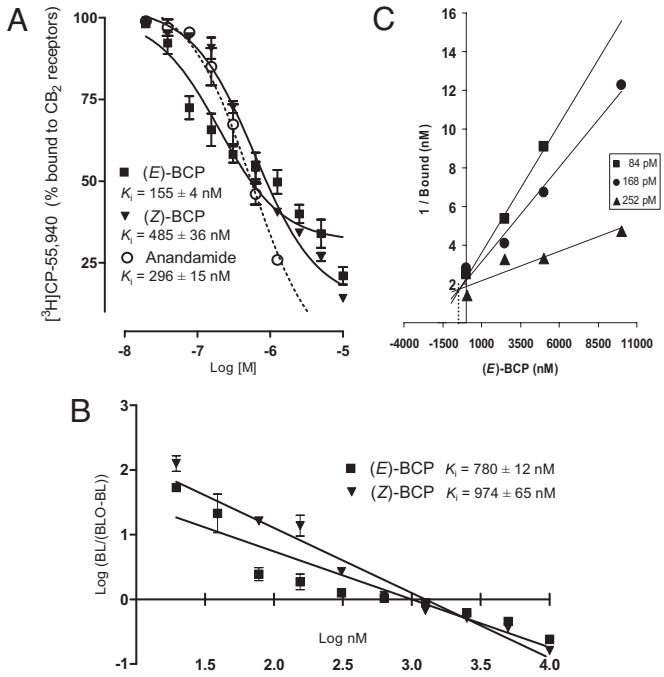

Fig. 2. (*E*)-BCP and (*Z*)-BCP displace [^{3}H]CP-55,940 from *h*CB_2 receptors expressed in HEK293 cells. (*A*) Sigmoidal displacement curves (R^2 = 0.93 for (*E*)-BCP and 0.98 for (*Z*)-BCP) show overall displacement (71% and 84%, respectively) with K_i values of 155 and 485 nM, respectively. Data show mean values of nine measurements ± SEM. (*B*) Hill plot showing linearized data and the corresponding K_i values. (*C*) Dixon plot of the competitive binding interaction of (*E*)-BCP with the CP-55,940 receptor binding site in the CB_2 receptor. Radioligand assays were performed by using 84 pM, 168 pM, and 252 pM [^{3}H]CP-55,940.

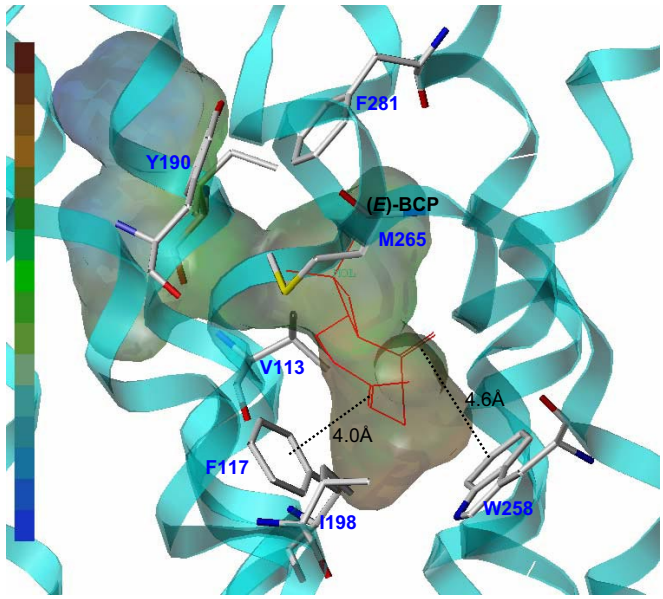

Fig. 3. Model of the putative interaction of (*E*)-BCP with the CB_2 receptor determined by Surflex–Dock and MD/MM calculations. (*E*)-BCP is located in the hydrophobic region of the amphipathic CB_2 receptor binding pocket where it closely interacts with hydrophobic residues F117, I198, W258, V113, and M265. In this model, significant π–π stacking interactions between the (*E*)-BCP double bonds and F117 and W258, respectively, facilitate binding.

receptor active compounds other than classical cannabinoids and that these ligands may also commonly occur in other plant species. Fractionation of *Cannabis* essential oil by column chromatography and screening of the isolated constituents yielded (*E*)-BCP as a CB_2 receptor binding compound (Fig. 1).

Quantitative radioligand binding experiments showed that (*E*)-BCP and its isomer, (*Z*)-BCP (Fig. 1), dose-dependently displaced [^{3}H]CP55,940 from *h*CB_2 receptors expressed in HEK293 cells with apparent K_i values in the nM range (Fig. 2*A*). (*E*)-BCP, which is the isomer predominantly found in plants, showed a slightly higher CB_2 receptor binding affinity (K_i = 155 ± 4 nM) than (*Z*)-BCP (K_i = 485 ± 36 nM). Notably, BCP oxide (Fig. 1), which is the volatile BCP oxidation product sensed by narcotic detection dogs (22), and the ring-opened isomer α-humulene did not displace [^{3}H]CP55,940 from the *h*CB_2 receptor ($K_i > 20$ μM) (Fig. S2). In accordance with the data obtained with *Cannabis* essential oils (Fig. S1), BCP isomers did not show significant binding affinity to the *h*CB_1 receptor (Fig. S2). Moreover, none of the other major *Cannabis* terpenes (10 μM) showed a significant displacement of [^{3}H]CP55,940 (> 50%) in either *h*CB_2 or *h*CB_1 receptor radioligand binding assays (Fig. S2).

(E)-BCP Competitively Binds to the *h*CB_2 Receptor THC Binding Site. Receptor binding studies were hampered by the poor water solubility of the apolar (*E*)-BCP (clogP = 6.7). (*E*)-BCP led to the formation of oil droplets at concentrations >1 μM, whereas (*Z*)-BCP showed a somewhat better water solubility (data not shown). Accordingly, the displacement curve for (*E*)-BCP showed a biphasic trend and K_i values for (*E*)-BCP and (*Z*)-BCP calculated from the Hill plot were 780 ± 12 nM and 974 ± 65 nM, respectively (Fig. 2*B*). Thus, the K_i values for (*E*)-BCP obtained in the nonlinear regression (Fig. 2*A*), and the Hill plot (Fig. 2*B*) showed a statistically significant 5-fold difference. Because the Hill plot for (*E*)-BCP deviates from linearity, the possibility of a biphasic nature of the displacement was explored by using the GraphPad Prism software. The biphasic displacement curve exhibited a poor correlation ($R^2 < 0.8$), suggesting that solubility rather than the presence of multiple binding sites was responsible for the discrepancy between K_i values from nonlinear regression analyses and Hill plots. This was subsequently confirmed in a Dixon analysis in which competitive binding of (*E*)-BCP to the CP55,940 binding site was shown (Fig. 2*C*). The inhibition constant estimated from the Dixon plot was ≈500 nM, again confirming the nanomolar range of the (*E*)-BCP binding affinity. Because THC and CP55,940 share the same binding site in the *h*CB_2 receptor, it can be concluded that (*E*)-BCP binds to the THC binding pocket or an overlapping site.

***In Silico* Docking Analysis of the (E)-BCP CB_2 Receptor Binding Interaction.** Computational docking analyses, using Surflex-Dock calculations (see *SI Materials and Methods*) with an established CB_2 receptor homology model (23), suggest that (*E*)-BCP binds into the hydrophobic region of the water-accessible cavity. The (*E*)-BCP-CB_2 complex energy was minimized by MD/MM simulations. The putative binding site of CB_2 receptor ligands is located adjacent to helices III, V, VI, and VII at the near extracellular site of the 7TM bundles (Fig. 3). In this model, the lipophilic (*E*)-BCP docks into the hydrophobic cavity of the amphiphatic binding pocket and the binding mode of (*E*)-BCP appears to be facilitated by π–π stacking interactions with residues F117 (4.0 Å) and W258 (4.6 Å). Moreover, (*E*)-BCP closely interacts with the hydrophobic residues I198, V113, and M265 (Fig. 3). Only four different geometries are allowed in (*E*)-BCP, owing to the constraints imposed by the nine-membered ring. These conformations are designated $\alpha\alpha$, $\alpha\beta$, $\beta\alpha$, and $\beta\beta$, showing the relative orientations of the C8-C13 exocyclic double bond and of the C4–C5 (–C12) vinylic moiety, in which α or β denotes the position of the C8–C13 double bond and the C12 methyl below or above the molecular plane (24). Based on the data obtained by molecular modeling, the bioactive conformation of (*E*)-BCP in the CB_2 receptor complex resembles the $\beta\beta$ low

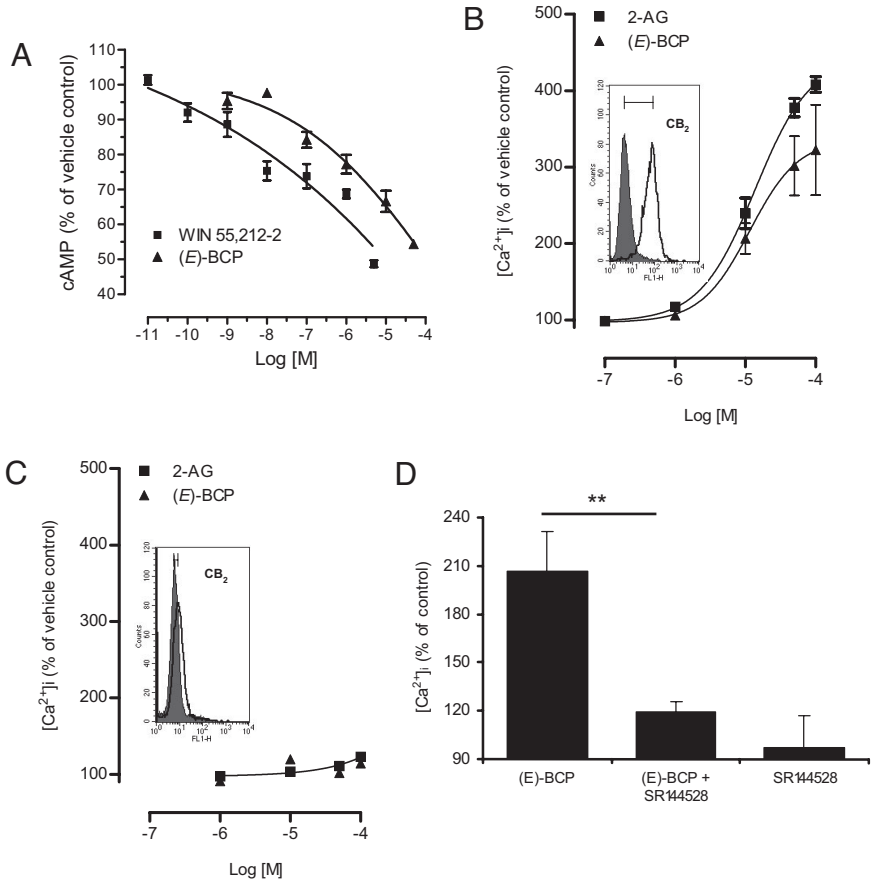

Fig. 4. G protein triggered effects of (*E*)-BCP upon CB_2 receptor binding. (*A*) The high-affinity CB ligand WIN55,212–2 and (*E*)-BCP dose-dependently inhibit forskolin-stimulated cAMP production in CB_2 receptor-transfected CHO-K1 cells. Data are mean values of three independent experiments measured in triplicates ± SEM in a nonlinear dose-response curve ($R^2 > 0.97$). (*B*) Like 2-AG, which was used as positive control, (*E*)-BCP dose-dependently triggers $[Ca^{2+}]_i$ transients in CB_2 expressing HL60 cells. The FACS histogram shows CB_2 immunofluorescence of HL60 cells. Data are mean values of three independent experiments ± SEM shown in a nonlinear dose-response curve ($R^2 = 0.99$). (*C*) No $[Ca^{2+}]_i$ transients were induced in HL60 cells devoid of CB_2 surface expression. The FACS histogram shows the lack of CB_2 Ab immunofluorescence in these HL60 cells. (*D*) Addition of the CB_2-selective antagonist SR144528 (1 μM) inhibited the $[Ca^{2+}]_i$ release triggered by (*E*)-BCP (10 μM) in CB_2-positive HL60 cells. Data are mean values from three independent experiments ± SEM (paired *t* test **, $P < 0.01$).

energy conformer (24). Because the Surflex-Dock scores are expressed in $-\log(K_d)$ units, the modeling results also indicate that (*E*)-BCP ($-\log(K_d) = 7.86$) and (*Z*)-BCP (7.96) exhibit >1,000-fold higher CB_2 receptor binding affinities than α-humulene (4.17), which is in agreement with the experimental data shown in Fig. S2.

(*E*)-BCP is a Full CB_2 Receptor Agonist Leading to G_i and G_o Signals. We next determined whether the interaction of (*E*)-BCP with the CB_2 receptor leads to G protein mobilization. Like the potent high-affinity cannabinoid ligand WIN55,212–2 (K_i *h*CB_2 = 1.2 nM) (21), (*E*)-BCP inhibited forskolin-stimulated cyclic adenosine monophosphate (cAMP) production in *h*CB_2 receptor transfected CHO-K1 cells (Fig. 4*A*). The difference in potency between WIN55,212-2 (EC_{50} = 38 ± 5.7 nM) and (*E*)-BCP (EC_{50} = 1.9 ± 0.3 μM) (Fig. 4*A*) reflects the ≈150-fold difference in CB_2 receptor binding affinity between these ligands. To assess whether (*E*)-BCP is a fully functional agonist at the CB_2 receptor, we measured CB_2-mediated intracellular calcium transients ($[Ca^{2+}]_i$) in promyelotic HL60 cells. Like the endocannabinoid 2-arachidonoylglycerol (2-AG), which is a potent activator of the G_o pathway that leads to $[Ca^{2+}]_i$ release (25), also (*E*)-BCP concentration-dependently triggered the release of $[Ca^{2+}]_i$ (Fig. 4*B*). The maximum increase in $[Ca^{2+}]_i$ of (*E*)-BCP (E_{max} = 312 ± 41%) was somewhat weaker than the maximum effect achieved with 2-AG (E_{max} = 409 ± 17%) (Fig. 4*B*). However, the E_{max} and EC_{50} values obtained in nonlinear regression analyses were not statistically different for 2-AG (EC_{50} = 13.8 ± 0.9 μM) and *E*-BCP (EC_{50} = 11.5 ± 2.8 μM). In HL60 cells devoid of CB_2 receptor surface expression *E*-BCP did not trigger $[Ca^{2+}]_i$ (Fig. 4*C*). Moreover, the $[Ca^{2+}]_i$ transients induced by (*E*)-BCP and 2-AG were fully blocked by the CB_2 receptor antagonist SR144528, which supports a strictly CB_2 receptor-dependent G_o mechanism of $[Ca^{2+}]_i$ release by (*E*)-BCP (Fig. 4*D*). BCP oxide induced significant $[Ca^{2+}]_i$ transients in CB_2 positive, but induced them even more strongly in CB_2 deficient HL60 cells (Fig. S3*A*), suggesting a CB_2 receptor-independent mechanism of action. As expected, this effect could not be inhibited by SR144528 (Fig. S3*B*). Because CB_2 receptor-selective agonists have been shown to increase phosphorylation of mitogen-activated protein (MAP) kinases p38 (26) and extracellular receptor kinases 1/2 (Erk1/2) (27), we incubated the CB_2 receptor-selective agonist JWH133 (K_i = 3.4 nM) and (*E*)-BCP with HL60 cells and human primary $CD14^+$ monocytes to determine the phosphorylation of these kinases upon CB_2 receptor activation. (*E*)-BCP and JWH133 (1 μM) led to rapid phosphorylation of Erk1/2 in both HL60 and primary $CD14^+$ monocytes, and this effect could be blocked by prior incubation with the CB_2 receptor antagonist SR144528 (Fig. S4). Although (*E*)-BCP weakly increased phosphorylated p38 in both HL60 cells and primary $CD14^+$ monocytes, JWH133 did not trigger p38 phosphorylation in primary $CD14^+$ monocytes.

(*E*)-BCP Inhibits Lipopolysaccharide (LPS)-Stimulated TNF-α and IL-1β Expression in Peripheral Blood. CB_2 receptor agonists have repeatedly been shown to inhibit the release of cytokines from LPS-stimulated monocytes, such as tumor necrosis factor-α (TNF-α) (14, 28, 29). To explore whether (*E*)-BCP triggers CB_2 receptor-dependent effects on cytokine expression *in vitro*, we measured cytokine levels in LPS-stimulated human whole blood after 18 h in the presence and absence of (*E*)-BCP. At 500 nM, (*E*)-BCP significantly inhibited LPS-stimulated IL-1β and TNF-α expression (Fig. 5*A*). This inhibition was clearly reversed by the CB_2 receptor-selective antagonist AM630 (5 μM), thus indicating a functional CB_2 receptor-dependent mechanism. AM630 was used because SR144528 potently inhibits cytokine expression in whole blood, as reported in ref. 29. As shown in Fig. 5*A*, the antiinflammatory effect

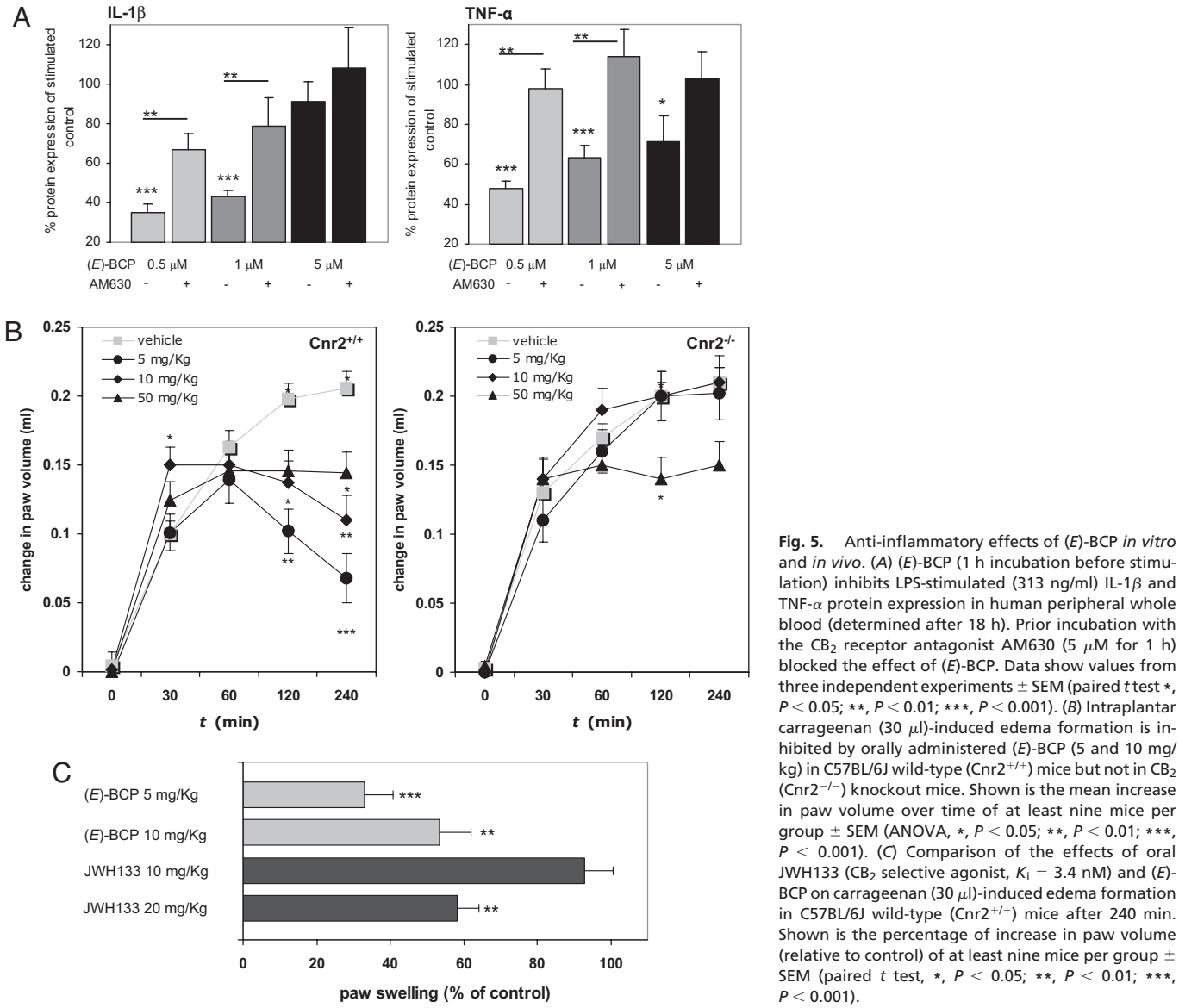

Fig. 5. Anti-inflammatory effects of (*E*)-BCP *in vitro* and *in vivo*. (*A*) (*E*)-BCP (1 h incubation before stimulation) inhibits LPS-stimulated (313 ng/ml) IL-1β and TNF-α protein expression in human peripheral whole blood (determined after 18 h). Prior incubation with the CB_2 receptor antagonist AM630 (5 μM for 1 h) blocked the effect of (*E*)-BCP. Data show values from three independent experiments ± SEM (paired *t* test *, $P < 0.05$; **, $P < 0.01$; ***, $P < 0.001$). (*B*) Intraplantar carrageenan (30 μl)-induced edema formation is inhibited by orally administered (*E*)-BCP (5 and 10 mg/kg) in C57BL/6J wild-type ($Cnr2^{+/+}$) mice but not in CB_2 ($Cnr2^{-/-}$) knockout mice. Shown is the mean increase in paw volume over time of at least nine mice per group ± SEM (ANOVA, *, $P < 0.05$; **, $P < 0.01$; ***, $P < 0.001$). (*C*) Comparison of the effects of oral JWH133 (CB_2 selective agonist, K_i = 3.4 nM) and (*E*)-BCP on carrageenan (30 μl)-induced edema formation in C57BL/6J wild-type ($Cnr2^{+/+}$) mice after 240 min. Shown is the percentage of increase in paw volume (relative to control) of at least nine mice per group ± SEM (paired *t* test, *, $P < 0.05$; **, $P < 0.01$; ***, $P < 0.001$).

was less pronounced with increasing concentrations of (*E*)-BCP, probably reflecting the formation of (*E*)-BCP aggregates or a weak simultaneous cellular stimulation of cytokines via a low-affinity target at μM concentrations. Below 500 nM, cytokine inhibition was concentration-proportional, and (*E*)-BCP produced less inhibition (data not shown). The LPS-stimulated expression levels of IL-6, -8, and -10 were not significantly influenced by (*E*)-BCP after 18 h (Fig. S5).

(*E*)-BCP Inhibits Lipopolysaccharide-Stimulated Erk1/2 and JNK1/2 Activation in Primary Monocytes. Based on the observation that (*E*)-BCP weakly induced p38 and Erk1/2 phosphorylation in primary $CD14^+$ monocytes and, at the same time, inhibits LPS-stimulated TNF-α and IL1β protein expression in whole blood, we investigated whether LPS-triggered p38, Erk1/2, and JNK1/2 activation was modulated by (*E*)-BCP. LPS stimulation of primary human monocytes led to a rapid and strong phosphorylation of p38 and JNK1/2, whereas a weaker activation of Erk1/2 was detected. Incubation of cells with (*E*)-BCP (500 nM) for 1 h before LPS stimulation led to a significant reduction of Erk1/2 and JNK1/2 activation (phosphorylation) as determined by Western blot (Fig. S6*A*) and cytometic bead array (CBA) analyses (Fig. S6*B*), whereas p38 activation was not influenced by (*E*)-BCP (data not shown).

Oral (*E*)-BCP Inhibits Carrageenan-Induced Edema in Wild Type Mice. To obtain *in vivo* evidence of the antiinflammatory effects induced by (*E*)-BCP *in vitro*, we examined the effectiveness of orally administered (*E*)-BCP in wild-type mice ($Cnr2^{+/+}$) and CB_2 receptor-deficient ($Cnr2^{-/-}$) mice. (*E*)-BCP (5 and 10 mg/kg) dosed orally significantly inhibited carrageenan-induced paw edema in wild-type mice by ≈70% and 50%, respectively (Fig. 5*B*). Somewhat unexpectedly, the lowest dose of (*E*)-BCP was most effective in this experiment (Fig. 5*B*). Because no antiinflammatory effect could be observed with the two lower doses of (*E*)-BCP in $Cnr2^{-/-}$ mice, the antiinflammatory effects of (*E*)-BCP in wild-type mice show that this natural product exerts CB_2 receptor-dependent cannabimimetic effects *in vivo*. Moreover, 10 mg/kg (*E*)-BCP showed an interesting biphasic effect, such that edema formation was augmented after 30 min relative to vehicle control but clearly inhibited after 120 min. This was not observed in $Cnr2^{-/-}$ mice, thus demonstrating that the CB_2 receptor is involved in both effects. Because 50 mg/kg (*E*)-BCP showed only a weak antiinflammatory

activity in both wild-type and Cnr2$^{-/-}$ mice (Fig. 5*B*), higher doses of (*E*)-BCP may lead to off-target effects. In comparison, the CB_2 receptor-selective agonist JWH133 (K_i = 3.4 nM) was significantly less effective in inhibiting carrageenan-induced edema formation than (*E*)-BCP after oral administration (Fig. 5*C*) despite its 45-fold higher CB_2 receptor affinity.

(*E*)-BCP Content in *Cannabis* Essential Oil Correlates with CB_2 Receptor Activation. (*E*)-BCP contents are known to vary in *Cannabis* strains and preparations (7), and we therefore analyzed five commercial *Cannabis* essential oils lacking classical cannabinoids by quantitative gas chromatography (GC). The percentage of (*E*)-BCP in the essential oils varied between 12.5 and 35% (Fig. S7). The (*E*)-BCP content in *Cannabis* essential oils positively correlated with the displacement of [^{3}H]CP55,940 and the amount of $[Ca^{2+}]_i$ triggered via CB_2 receptors in HL60 cells (Fig. S7), thus confirming that this natural product is the only cannabimimetic in *Cannabis* essential oil.

Discussion

The abundant plant sesquiterpene (*E*)-BCP is shown to competitively interact with the CP55,940 binding site (i.e., THC binding site) of the peripheral *h*CB_2 cannabinoid receptor with a K_i value in the nanomolar range (Fig. 2). Results from molecular modeling studies suggest that (*E*)-BCP binds to a previously described putative ligand binding pocket in the *h*CB_2 receptor (Fig. 3) (29). Although other ligands like *N*-alkylamides may span the entire amphiphatic binding pocket or bind adjacent to the water accessible cavity (e.g., close to Y190) (29), (*E*)-BCP binds to the hydrophobic cavity, where it interacts with hydrophobic residues F117, I198, W258, V113, and M265 (Fig. 3). The C4–C5 double bond in (*E*)-BCP exhibits a π–π stacking interaction with F117 (4.0 Å), and thus its geometry likely plays an important role for *h*CB_2 receptor binding. This hypothesis is in line with the experimental difference in CB_2 receptor binding between (*E*)-BCP and (*Z*)-BCP (Fig. 2) and the loss of binding affinity of BCP oxide (Fig. S2). (*E*)-BCP activation of the *h*CB_2 receptor triggers a full stimulation program, involving inhibition of cAMP, stimulation of $[Ca^{2+}]_i$ transients, and weak activation of the MAP kinases p38 and Erk1/2 (Fig. 4 and Fig. S4). Like other CB_2 receptor-selective agonists, (*E*)-BCP leads to antiinflammatory effects *in vitro* and *in vivo* (Fig. 5). An inhibition of LPS-stimulated TNF-α and IL-1β expression (Fig. 5*A*) is typically exerted by CB receptor ligands, such as CB_2 receptor agonists (14, 28, 29). However, the underlying molecular mechanism of this effect remains to be elucidated. Our data suggest that a CB_2 receptor-mediated suppression of Erk1/2 and JNK1/2 signaling is involved (Fig. S6). Because Erk1/2 and JNK1/2 signaling pathways are critical for LPS-stimulated expression of IL-1 and TNF-α (30), CB_2 receptor ligands capable of inhibiting the activation of these kinases may down-regulate IL-1β and TNF-α expression. Data have shown (15) that different CB_2 receptor-selective ligands, including CB_2 receptor agonists, are able to inhibit carrageenan-stimulated edema formation in mice. Our results on the (*E*)-BCP-mediated inhibition of carrageenan-stimulated edema in wild-type but not (Cnr2$^{-/-}$) mice (Fig. 5*B*) are in agreement with these data. Somewhat paradoxically, activation of the CB_2 receptor has also been shown to exert proinflammatory effects in the periphery, such as in the skin (31, 32). Thus, different cell types and the context of stimulation appear to mediate distinctly different CB_2 receptor-dependent immunomodulatory effects. This is also shown by our data, where (*E*)-BCP in monocytes activates constitutive Erk1/2 (Fig. S4) but inhibits LPS-stimulated Erk1/2 (Fig. S6). Whether the inverse dose-dependency of (*E*)-BCP and the initial increase in edema formation in wild-type mice at 10 mg/kg reflect the action of differentially activated G protein subsets needs to be elucidated. However, in the carrageenan model of acute inflammation, low doses of (*E*)-BCP are clearly antiinflammatory (Fig. 5*B*). Moreover, in this model, (*E*)-BCP is more potent than the high-affinity CB_2 receptor-selective agonist JWH133 (Fig. 5*C*). (*E*)-BCP has been reported to exert diverse antiinflammatory effects *in vivo* (33, 34), including gastric antiinflammatory and cytoprotective effects. These findings are in agreement with the pharmacology of CB_2 receptor agonists (35–37). In a recent report (38), (*E*)-BCP and α-humulene were shown to be orally available inhibitors of histamine-triggered edema and inflammation in mice with equipotent effects as dexamethasone. Although the molecular basis for these findings was not elucidated in this previous work, it is clear from our own studies that α-humulene does not interact with the CB_2 receptor (Fig. S2). Thus, it is possible that the *in vivo* effects of macrocyclic sesquiterpenes may not be exclusively mediated through the CB_2 receptor, which also appears to be supported by the carrageenan experiments with 50 mg/kg oral (*E*)-BCP (Fig. 5*B*). However, although other yet unknown targets may be involved, the antiinflammatory effects of the low oral doses of (*E*)-BCP are directly related to CB_2 receptor activation, because (*E*)-BCP is ineffective in (Cnr2$^{-/-}$) mice (Fig. 5*B*).

(*E*)-BCP is the first *Cannabis*-derived functional CB receptor ligand with a fundamentally different structure from the classical cannabinoids. Thus, it represents a new type of CB_2 receptor-selective agonist that is based on an unusual cyclobutane-containing scaffold. Recently (39), a *Cannabis* extract (Sativex) was approved in Canada for the treatment of neuropathic pain in multiple sclerosis. Because (*E*)-BCP is a major constituent in *Cannabis* essential oil (Fig. S7) and shows significant cannabimimetic effects, it may also contribute to the overall effect of *Cannabis* preparations, including Sativex. Moreover, (*E*)-BCP is commonly ingested with vegetable food, and an estimated daily intake of 10–200 mg of this lipophilic sesquiterpene could be a dietary factor that potentially modulates inflammatory and other pathophysiological processes via the endocannabinoid system. Consequently, the pharmacokinetics of (*E*)-BCP in humans and its potential impact on health should be addressed in future studies.

Materials and Methods

Drugs and Antibodies. See *SI Materials and Methods*.

Data Analysis. Results are expressed as mean values ± SD or ± SEM for each examined group. Statistical significance of differences between groups was determined by the Student's *t* test (paired *t* test) with GraphPad Prism4 software. Outliners in a series of identical experiments were determined by Grubb's test (ESD method) with alpha set to 0.05. Statistical differences between treated and vehicle control groups were determined by Student's *t* test for dependent samples. For animal experiments, statistical differences between treated and vehicle control groups were determined by repeated measurements (ANOVA) and post hoc least square difference tests. Differences between the analyzed samples were considered as significant at $P \leq 0.05$. Nonlinear regression analysis (curve fitting) was performed with GraphPad Prism4 software.

Cell Cultures. See *SI Materials and Methods*.

FACS Analysis of CB_2 Expression. Cellular surface expression of the CB_2 receptor was quantified by immunofluorescence as described in ref. 29 (for additional details, see *SI Materials and Methods*).

Radioligand Displacement Assays on CB_1 and CB_2 Receptors. [^{3}H]CP-55,940 binding and displacement experiments were performed as described in ref. 29. (For additional details, see *SI Materials and Methods*.) Data were fitted in a sigmoidal curve and graphically linearized by projecting Hill plots, which for both cases allowed the calculation of IC_{50} values. Derived from the dissociation constant (K_D) of [^{3}H]CP-55,940 (0.39 nM) and the concentration-dependent displacement (IC_{50} value), inhibition constants (K_i) of competitor compounds were calculated by using the Cheng–Prusoff equation [$K_i = IC_{50}/(1 + L/K_D)$] (40).

Molecular Modeling. The CB_2 receptor homology model used for molecular modeling was described in ref. 23. Docking of (*E*)-BCP, (*Z*)-BCP and α-humulene and CB_2 protein-ligand complex MD/MM studies were performed on the basis of published docking protocols, using Tripos molecular modeling packages Sybyl7.3.3 and Tripos force field (23, 29). (For additional details, see *SI Materials and Methods*.)

cAMP Assay. Human CB_2-receptorexpressing CHO-K1 cells were plated in 96-well plates at a density of 3×10^5 cells per ml and incubated overnight. After aspirating the media, the cells were chilled for 10 min at room temperature in RPMI medium 1640 (w/o supplements) containing 500 μM 3-isobutyl-1-methylxanthine. Cells were then treated with different concentrations of test-compounds and incubated for 30 min at 37°C in a total volume of 100 μl. After another 30 min of incubation at 37°C with 20 μM forskolin, intracellular cAMP levels were detected by HitHunter for adherent cells EFC chemiluminescent detection assay (Amersham; catalog no. 90000302) according to the manufacturer's instructions and measured on a Microlumat *Plus* Microplate Luminometer LB 96V (EG&G Berthold). The high-affinity CB receptor ligand WIN55,212–2 was used as positive control.

Measurement of $[Ca^{2+}]_i$. Intracellular Ca^{2+} was quantified in HL60 cell lines by FACS measurements as described in ref. 29. (For additional details, see *SI Materials and Methods*.)

CBA Quantification of Cytokines in Human Blood Plasma. Human peripheral whole blood cultures were obtained as described in ref. 29. Cytokine production in human peripheral whole blood was analyzed in blood plasma of whole blood cultured for 18 h at 37°C, 5% CO_2, using Cytometric Bead Arrays (BD Biosciences; human inflammation CBA kit 551811) as described in ref. 29. (For additional details, see *SI Materials and Methods*.)

Determination of p38, Erk1/2, and JNK1/2 Activation. Phsophorylation of p38 and Erk1/2 was analyzed in HL60 CB_2-positive cells and $CD14^+$ peripheral blood mononuclear cells (PBMCs). PBMCs were isolated from human buffy coats by density gradient centrifugation as reported in ref. 29. Phosphoproteins were quantified with CBA Phospho p38 MAPK Flex Set 560010 (T180/T182), Phospho Erk1/2 Flex Set 560012 (T202/Y204), and the Phospho JNK1/2 Flex Set (T183/Y185) from BD Biosciences according to the manufacturer's instructions.

Western Blot Analysis. Western blots were carried out by standard methods (see *SI Materials and Methods*).

Animals. Male CB_2 knockout mice ($Cnr2^{-/-}$) on a C57BL6/J congenic background (32) and their C57BL6/J ($Cnr2^{+/+}$) wild-type controls ≈3 months of age were used. Animals were housed in groups of 3–5 and had access to water and food ad libitum. The housing conditions were maintained at 21 ± 1°C and 55 ± 10% relative humidity in a controlled light–dark cycle (light on between 7:00 a.m. and 7:00 p.m.). All experimental procedures and animal husbandry were conducted according to standard ethical guidelines.

Animal Treatment. (*E*)-BCP was dissolved in olive oil (Fluka) and gavage-fed to the animals (with the help of feeding needle) 30 min (50 mg/kg) and 60 min (5 and 10 mg/kg) before carrageenan treatment. Olive oil without (*E*)-BCP was gavage-fed to the animals as vehicle control.

Carrageenan–Paw Edema. The experiments were performed as described in ref. 41. Briefly, Carrageenan (2%, 20 mg/ml suspended in saline; Sigma) was injected intraplantar in a volume of 30 μl into the hind right paw, using a 27-gauge needle. The left paw received the same amount of saline and it was used as control. Edema was measured by using a Volume meter (TSE) at a several time points after carrageenan injection. Edema was expressed in milliliters as the difference between the right and left paw.

GC Measurements. Gas chromatography measurements were carried out as described in the European Pharmacopoeia 5.5 (Pinus silvestris oil) with a Thermo Electron Focus GC instrument (Thermo Fisher Scientific) fitted with a BGB wax column (60 m, 0.25-mm diameter, 0.25-μm film; serial no. 13651937). (For additional details, see *SI Materials and Methods*).

ACKNOWLEDGMENTS. We thank Dr. Irmgard Werner and Alex Hermann for their help and technical assistance for the GC measurements, Andreas Nievergelt-Meier for his help with the CBA analyses, and Dr. Michael Detheux (Euroscreen S.A., Brussels, Belgium) for the CB_2-transfected CHO-K1 cell line. This work was supported by the Deutsche Forschungsgemeinschaft Grants FOR926 and GRK804.

1. Pichersky E, Noel JP, Dudareva N (2006) Biosynthesis of plant volatiles: Nature's diversity and ingenuity. *Science* 311:808–811.
2. Rasmann S, *et al.* (2005) Recruitment of entomopathogenic nematodes by insect-damaged maize roots. *Nature* 434:732–737.
3. Orav A, Stulova I, Kailas T, Müürisepp M (2004) Effect of storage on the essential oil composition of Piper nigrum L. fruits of different ripening states. *J Agric Food Chem* 52:2582–2586.
4. Jayaprakasha GK, Jagan Mohan Rao L, Sakariah KK (2003) Volatile constituents from Cinnamomum zeylanicum fruit stalks and their antioxidant activities. *J Agric Food Chem* 51:4344–4348.
5. Mockute D, Bernotiene G, Judzentiene A (2001) The essential oil of Origanum vulgare L. ssp. vulgare growing wild in vilnius district (Lithuania). *Phytochemistry* 57:65–69.
6. Sköld M, Karlberg AT, Matura M, Börje A (2006) The fragrance chemical beta-caryophyllene-air oxidation and skin sensitization. *Food Chem Toxicol* 44:538–545.
7. Hendriks H, Malingre T, Battermann S, Boss R (1975) Mono- and sesquiterpene hydrocarbons of the essential oil of Cannabis sativa. *Phytochemistry* 14:814–815.
8. Pertwee RG (2007) The diverse CB(1) and CB(2) receptor pharmacology of three plant cannabinoids: Delta(9)-tetrahydrocannabinol, cannabidiol and Delta(9)-tetrahydrocannabivarin. *Br J Pharmacol* 53:199–215.
9. Matsuda LA, Lolait SJ, Brownstein MJ, Young AC, Bonner TI (1990) Structure of a cannabinoid receptor and functional expression of the cloned cDNA. *Nature* 346:561–564.
10. Munro S, Thomas KL, Abu-Shaar M (1993) Molecular characterization of a peripheral receptor for cannabinoids. *Nature* 365:61–65.
11. Mackie K (2006) Cannabinoid receptors as therapeutic targets. *Annu Rev Pharmacol Toxicol* 46:101–122.
12. Devane WA, *et al.* (1992) Isolation and structure of a brain constituent that binds to the cannabinoid receptor. *Science* 258; 1946–1949.
13. Sugiura T, Waku K (2000) 2-Arachidonoylglycerol and the cannabinoid receptors. *Chem Phys Lipids* 108:89–106.
14. Klein TW (2005) Cannabinoid-based drugs as anti-inflammatory therapeutics. *Nat Rev Immunol* 5:400–411.
15. Iwamura H, Suzuki H, Kaya T, Inaba T (2001) In vitro and in vivo pharmacological characterization of JTE-907, a novel selective ligand for cannabinoid CB2 receptor. *J Pharmacol Exp Ther* 296:420–425.
16. Ibrahim MM, *et al.* (2005) CB2 cannabinoid receptor activation produces antinociception by stimulating peripheral release of endogenous opioids. *Proc Natl Acad Sci USA* 102:3093–3098.
17. Batkai S, *et al.* (2007) Cannabinoid-2 receptor mediates protection against hepatic ischemia/reperfusion injury. *FASEB J* 21:1788–1800.
18. Kimball ES, Schneider CR, Wallace NH, Hornby PJ (2006) Agonists of cannabinoid receptor 1 and 2 inhibit experimental colitis induced by oil of mustard and by dextran sulfate sodium. *Am J Physiol Gastrointest Liver Physiol* 291:G364–371.
19. Steffens S, *et al.* (2005) Low dose oral cannabinoid therapy reduces progression of atherosclerosis in mice. *Nature* 434:782–786.
20. Ofek O, *et al.* (2006) Peripheral cannabinoid receptor, CB2, regulates bone mass. *Proc Natl Acad Sci USA* 103:696–701.
21. Mukherjee S, *et al.* (2004) Species comparison and pharmacological characterization of rat and human CB2 cannabinoid receptors. *Eur J Pharmacol* 505:1–9.
22. Stahl E, Kunde P (1973) Die Leitsubstanzen der Haschisch-Suchhunde [Leading substances for hashish narcotic dogs]. Kriminalistik, 9:385–388.
23. Chen JZ, Wang J, Xie X-Q (2007) GPCR structure-based virtual screening approach for CB2 antagonist search. *J Chem Inf Model* 47:1626–1637.
24. Clericuzio M, Alagona G, Ghio C, Toma L (2000) Ab initio and density functional evaluations of the molecular conformations of beta-caryophyllene and 6 hydroxy-caryophyllene. *J Org Chem* 65:6910–6916.
25. Shoemaker JL, Buckle MB, Mayeux PR, Prather PL (2005) Agonist-directed trafficking of response by endocannabinoids acting at CB2 receptors. *J Pharmacol Exp Ther* 315:828–838.
26. Herrera B, Carracedo A, Diez-Zaera M, Guzmán M, Velasco G (2005) p38 MAPK is involved in CB2 receptor-induced apoptosis of human leukaemia cells. *FEBS Lett* 579:5084–5088.
27. Correa F, Mestre L, Docagne F, Guaza C (2005) Activation of cannabinoid CB2 receptor negatively regulates IL-12p40 production in murine macrophages: Role of IL-10 and ERK1/2 kinase signaling. *Br J Pharmacol* 145:441–448.
28. Klegeris A, Bissonnette CJ, McGeer PL (2003) Reduction of human monocytic cell neurotoxicity and cytokine secretion by ligands of the cannabinoid-type CB2 receptor. *Br J Pharmacol* 139:775–786.
29. Raduner S, *et al.* (2006) Alkylamides from Echinacea are a new class of cannabinomimetics. Cannabinoid type 2 receptor-dependent and -independent immunomodulatory effects. *J Biol Chem* 281:14192–14206.
30. Guha M, Mackman N (2001) LPS induction of gene expression in human monocytes. *Cell Signal* 13:85–94.
31. Oka S, *et al.* (2006) Involvement of the cannabinoid CB2 receptor and its endogenous ligand 2 arachidonoylglycerol in oxazolone-induced contact dermatitis in mice. *J Immunol* 177:8796–8805.
32. Karsak M, *et al.* (2007) Attenuation of allergic contact dermatitis through the endocannabinoid system. *Science* 316:1494–1497.
33. Martin S, *et al.* (1993) Anti-inflammatory activity of the essential oil of Bupleurum fruticescens. *Planta Med* 59:533–536.
34. Cho JY, *et al.* (2007) Amelioration of dextran sulfate sodium-induced colitis in mice by oral administration of beta-caryophyllene, a sesquiterpene. *Life Sci* 80:932–939.
35. Tambe Y, Tsujiuchi H, Honda G, Ikeshiro Y, Tanaka S (1996) Gastric cytoprotection of the non-steroidal anti-inflammatory sesquiterpene, beta-caryophyllene. *Planta Med* 62:469–470.
36. Thuru X, *et al.* (2007) Cannabinoid receptor 2 is required for homeostatic control of intestinal inflammation. *17th Annual Symposium on the Cannabinoids* (International Cannabinoid Research Society, Burlington, VT), p 19. Available at www.cannabinoid-society.org/symposium.2007/2007.icrs.program.and.abstracts.pdf.
37. Di Marzo V, Izzo A (2006) Endocannabinoid overactivity and intestinal inflammation. *Gut* 55:1373–1376.
38. Fernandes ES, *et al.* (2007) Anti-inflammatory effects of compounds alpha-humulene and (−)-trans-caryophyllene isolated from the essential oil of Cordia verbenacea. *Eur J Pharmacol* 569:228–236.
39. Russo EB, Guy GW, Robson PJ (2007) Cannabis, pain, and sleep: Lessons from therapeutic clinical trials of Sativex, a cannabis-based medicine. *Chem Biodivers* 4:1729–1743.
40. Cheng YC, Prusoff WH (1973) Relationship between the inhibition constant (K1) and the concentration of inhibitor which causes 50 per cent inhibition (I50) of an enzymatic reaction. *Biochem Pharmacol* 22:3099–3108.
41. Mogil JS, *et al.* (1999) Heritability of nociception I: Responses of 11 inbred mouse strains on 12 measures of nociception. *Pain* 80:67–82.